Molecular Omics

ROYAL SOCIETY OF CHEMISTRY

RESEARCH ARTICLE

View Article Online
View Journal

Cite this: DOI: 10.1039/d4mo00140k

Differential modulation of the hepatocellular metabolome, cytoprotective and inflammatory responses due to endotoxemia and lipotoxicity†

Jyoti Sharma and Priyankar Dey *

Received 20th September 2024,
Accepted 16th December 2024

DOI: 10.1039/d4mo00140k

rsc.li/molomics

The present work aimed to examine the primary mechanisms of liver damage, namely the impact of gut-derived endotoxins along the gut–liver axis and adipose-derived free fatty acids along the adipose–liver axis. These processes are known to play a significant role in the development of hepatic inflammation and steatosis. Although possible overlapping in the pathogenesis was expected, these processes have unique pathophysiological consequences. Therefore, we used HepG2 cells as a model system to investigate the impact of lipopolysaccharides (LPS) and free fatty acid (FFA; albumin conjugated palmitic acid) on the intracellular metabolome. Although both LPS and FFA triggered the expression of nuclear factor κB (NFκB)-dependent inflammation, only LPS treatment was able to trigger a Toll-like receptor 4 (TLR4) dependent response. The intracellular cytoprotective enzymatic levels (catalase, peroxidase, glutathione) were increased due to FFA but lowered due to LPS. The free-radical neutralizing efficacies of cell-free metabolites of FFA-treated cells were better than those of the LPS-treated ones. The use of untargeted metabolomics allowed for the identification of distinct metabolic pathway enrichments, providing further insights into the differential effects of LPS and FFA on the metabolism of hepatocytes. Collectively, the current study highlights the distinct impacts of endotoxemia and lipotoxicity on the metabolome of hepatocytes, hence offering valuable insights into hepatocellular function.

1. Introduction

The liver is crucial for maintaining overall metabolic homeostasis by regulating nutrient metabolism and storage, drug detoxification, and energy homeostasis. Numerous conditions are linked to liver injury, including autoimmune diseases, viral infections, consequences from drugs and alcohol, and metabolic diseases like diabetes, obesity, and metabolic dysfunction-associated liver disease (MASLD). In particular, MASLD is characterized by a prevalence of both lipotoxicity and endotoxemia-associated hepatic insults, which range from simple steatosis to cirrhosis and may eventually result in hepatocellular cancer.[1,2] Due to the increased prevalence of metabolic syndrome in relation to calorie intake and sedentary lifestyle, the prevalence of the MASLD spectrum is surpassing the rate of viral or alcohol-induced liver diseases, even though historically, viral liver diseases accounted for the largest share of liver disease-related mortality.[3,4]

While various environmental (*e.g.*, diet and lifestyle) and genetic factors may contribute to MASLD, endotoxemia and lipotoxicity along the gut–liver and adipose–liver axis play critical roles in the promotion and progression of MASLD.[5,6] The translocation of gut microbial pyrogenic products along the gut–liver axis through a 'leaky-gut' results in the activation of hepatic Kupffer cells.[7] Elevation of endotoxin in both serum and the liver was reported in multiple cohorts of patients with metabolic liver disease.[8,9] Indeed, experimental evidence shows that reduction in endotoxin translocation along the gut–liver axis could attenuate metabolic syndrome-associated MASLD,[10] while hepatic loss-of-function of Toll-like receptor 4/nuclear factor κB (TLR4/NFκB) signaling protects mice from diet-induced MASLD.[11] Another mode of hepatic insult is associated with lipotoxicity due to adipose lipolysis and translocation of adipose-derived free non-esterified fatty acid along the adipose–liver axis, triggering hepatic steatosis.[12] Additionally, lipotoxicity caused by *de novo* lipogenesis and the formation of reactive lipid intermediates trigger oxidative damage and inflammation in the liver.[13] Gut-derived endotoxin affects hepatic lipid accumulation *via* inducing adipose lipolysis in addition to directly causing liver inflammation.[14] Indeed, the liver is considered the primary afflicted organ due to gut-derived endotoxin translocation, whereas adipose lipolysis

Department of Biotechnology, Thapar Institute of Engineering and Technology, Patiala, Punjab, India. E-mail: priyankar.dey@thapar.edu, priyankardey28@gmail.com; Tel: +91-9064275660

† Electronic supplementary information (ESI) available. See DOI: https://doi.org/10.1039/d4mo00140k

can result in hepatic steatosis.[15] Since the pathophysiological effects of endotoxemia and lipotoxicity are different, they are often regarded as separate causes of liver damage; nonetheless, when combined, they result in hepatic metainflammation. However, there is a severe shortage of experimental data to comprehend the separate hepatocellular response to lipotoxicity and endotoxemia. In fact, due to the recent increased prevalence of lean MASLD, a condition that is not associated with obesity and adipose-derived lipotoxicity,[16,17] understanding to what extent these individual modes of injury affect the hepatocellular immunometabolic homeostasis remains crucial.

In recent years, systemic and tissue-specific metabolites have been used as prognostic markers for early detection of chronic disease. Metabolomics strategies have been used in liver disease for multiple purposes, including marker identification for MASLD,[18] cirrhosis,[19] hepatocellular carcinoma,[20] and to differentiate between various stages of the MASLD spectrum.[21,22] In fact, metabolome-based rapid diagnostic approaches are emerging popular strategies in disease-associated biomarker discovery, drug development, understanding disease mechanisms, characterizing disease subtypes, predicting disease risk, monitoring treatment response, nutritional assessment, metabolic disorders, and microbiome research.[22–25] Nevertheless, to our knowledge, the independent effects of endotoxemia and lipotoxicity on the hepatocellular metabolome have never been comparatively studied before. Therefore, in the present study, by utilizing HepG2 cells, the independent effects of LPS and fatty acid on the intracellular metabolome were evaluated. The resultant metabolites were mapped against appropriate cellular pathways. Collectively, the results, for the first time, demonstrate how LPS and fatty acid differentially impact the overall intracellular metabolic homeostasis of HepG2 cells.

2. Materials and methods

2.1. Preparation of the fatty acid–albumin conjugate

Palmitic-acid albumin conjugate was prepared based on a previously standardized method.[26] The choice of palmitic acid was based on the fact that it is the predominant fatty acid in the serum of MASLD patients[27] and the superior effects of palmitic acid over other fatty acids in inducing hepatocellular ROS generation, inflammation, and cell death.[28–30] In brief, palmitic acid (Sigma #P0500) was heated at 70 °C with 0.1 M NaOH under constant shaking in a Thermo mixer to prepare a stock solution (0.1 M, solution A). In parallel, 5% (w/v) FAA and endotoxin-free bovine serum albumin (Sigma #126579) were mixed with water at 55 °C under constant shaking (solution B). Both the solutions were mixed at the desired proportions at 55 °C under constant shaking to obtain 10 mM PA–BSA conjugate. The resultant was filtered through a 0.45 μM hydrophilic membrane syringe filter, cooled down at room temperature, and stored at −20 °C until further use (stability 3–4 weeks).

2.2. HepG2 cell culture

HepG2 cells were procured from the National Institute of Cell Science (Pune, India) and were cultured as per our previously standardized method.[31] In brief, cells were cultured (37 °C and 5% CO_2) in low-glucose Dulbecco's modified Eagle medium (HiMedia, India) supplemented with 10% fetal bovine serum, 100 UI mL^{-1} penicillin, 100 μg mL^{-1} streptomycin, and 25 μg mL^{-1} amphotericin B. An Olympus inverted microscope (model) was used to track cell development during subculturing, which was carried out at intervals of 45–50 h. Cell counting equipment (Far-scope B, Curiosis) was used to do the trypan blue cell count.

2.3. Cytotoxicity test

For dose selection of LPS and FFA, a 3-(4,5-dimethylthiazol-2-yl)-2,5-diphenyl-2*H*-tetrazolium bromide (MTT) cell viability assay was performed, as described previously.[32] In brief, cells were seeded in the wells of a 96-well plate for 24 h to achieve 75–80% confluency. Then, the cells were either treated with LPS (0–800 μg mL^{-1}, *E. coli* 055: B5, Sigma #L2637) or FAA (0–1600 μM) to a final volume of 250 μL and incubated for 24 h. After incubation, 200 μL of the culture supernatant was removed carefully and 5 μg mL^{-1} of MTT solution (20 μL) was added to each well, and the plate was incubated for 4 h in the dark. After incubation, 150 μL of DMSO was added to each well, mixed well, and the absorbance was read at 540 nm against a suitable blank. Cells were cultured for 48 h to study the time-dependent effects of LPS and FFA on the cells.

2.4. *In vitro* experimental design

HepG2 cells were seeded in 6 well-plates (2×10^6 cells per mL) in DMEM without serum for 24-h to achieve 85–90% confluency. Next, the cells were either treated with FAA-albumin conjugate at 400 μM concentration or with 200 ng mL^{-1} lipopolysaccharide (LPS; *E. coli* O55.B5, Sigma, USA) for 24 h under standard conditions. Untreated cells were considered as a control. After 24-h of treatment, the cells were separated from the culture supernatant and cell extracts were prepared as described before.[31]

2.5. Intracellular metabolome

HepG2 cells were cultured for 48 h as described and then centrifuged (5000 rpm for 10 min) to isolate the cell pellet.[33] The cells were washed twice with PBS. The cell pellet was resuspended in chilled methanol : water (3 : 1, v/v) and vortexed vigorously for 15 min, then centrifuged at 10 000 rpm for 10 min at 4 °C. The supernatant was passed through a 0.4 μm filter to remove cells, and the filtrate was collected in a separate vial, dried under N_2, and then mixed with 20 μl of *N*,*O*-bis(trimethylsilyl)trifluoroacetamide + trimethylchlorosilane (99 : 1 v/v) mixture and incubated for 60 min at 25 °C with occasional vortexing, and then sealed in autosampler vials with a polytetrafluoroethylene cap using N_2 flushing.[34] Pooled metabolite extract (n = 3) was analyzed using a Shimadzu QP 2010 Ultra GC-MS instrument equipped with a TG-5MS column

(30 m × 0.25 mm × 0.25 μm). The injector temperature was set at 250 °C and the initial temperature of the program was set at 60 °C (solvent delay 4 min) with a hold of 4 min, followed by a ramp of 10 °C to 300 °C with a hold of 10 min. Derivatized samples (1 μL) were injected in a split mode (split ratio 20 : 1) with a splitless time of 0.80 min, with a constant flow of helium gas (1 mL min^{-1}). The MS transfer line temperature was set at 290 °C with an ion-source temperature of 200 °C (electron ionization). The samples were analyzed at electron energy 70 eV (vacuum pressure: 2.21 × $10^{-0.5}$ torr), and the mass analyzer range was set to 50–650 amu. MS data were analyzed using automated mass spectral deconvolution and identification system (AMDIS) version 2.70. The major and essential compounds were identified by mass fragmentation patterns (*m*/*z*) of the reference parent compound (molecular peak and base peak) using MS Interpreter version 2.0 and by matching with the reference database of the National Institute Standard and Technology (NIST) with an MS Library V2011.

2.6. Intracellular metabolic pathway prediction

MetaboAnalyst V5 was used to analyze the biochemical pathway enrichment using the metabolite abundance data sets obtained from the GC-MS analysis.[35,36] Enrichment analysis was performed based on the small molecule pathway database (SMPDB) and was used to investigate how groups of functionally related metabolites are significantly enriched that would potentially eliminate requirements of preselect compounds based on arbitrary cut-off thresholds. Identified metabolites were mapped against PubChem and SMPDB identifiers. Pathway analysis was performed based on SMPDB identifiers, where out-degree centrality was used for topology analysis, and Fisher's exact test was used as the enrichment method.

2.7. RNA extraction and gene expression

Gene expression study was performed following our previous method.[37,38] In brief, after appropriate treatment, cells were centrifuged at 5000 × *g* for 10 min to separate them from the culture media. The cell pellet was washed twice with ice-cold PBS to remove residual media components. Total mRNA from the HepG2 cells was extracted using the TRIZOL reagent (ThermoFisher Scientific) method according to the manufacturer's instructions, and quantification was done in nanodrop (Thermo Scientific). cDNA was synthesized using an iScript reverse transcription kit, and gene expression studies were performed using an SYBR green PCR kit on a real-time instrument (Bio-Rad, CFX96). Primer sequences are given in Table 1.

Table 1 Sequence of qRT-PCR primers

Gene name	Forward primer	Reverse primer
TNFα	AGCCCATGTTGTAGCAAACC	GGAAGACCCCTCCCAGATAG
TLR4	GCAATGGATCAAGGACCAGA	CTACAAGCACACTGAGGACC
IL1β	ACGAATCTCCGACCACCACTA	TCCATGGCCACAACAACTGAC
MyD88	GACCCCTGGTGCAAGTACC	AGTAGCTTACAACGCATGACAG
18S	CGCTTCCTTACCTGGTTGAT	GAGCGACCAAAGGAACCATA

Target genes were quantified relative to 18S using the $2^{-\Delta\Delta CT}$ method.

2.8. Biochemical assays

After treating for 24-h with LPS or FAA, the media was removed and cells were washed twice in PBS. Cells were then lysed using chilled lysis buffer, centrifuged at 10 000 rpm (10 min, 4 °C). The supernatant was split into multiple aliquots and used in enzymatic assays. First, the influence of the cell extracts on the oxidation of guaiacol was spectrometrically measured at 436 nm to determine the level of peroxidase as described before.[39] The level of cellular catalase was measured by evaluating the breakdown of H_2O_2 at 240 nm using the standard method.[31] GSH (LifeSpan BioSciences) and lipid peroxidation (RayBiotech) were measured in the cell lysate using a commercially available kit.

2.9. Nitrite estimation assay

The level of nitrite released in the culture supernatant was measured using the Griess reagent method as described previously.[32] In brief, culture supernatant (50 μL) was mixed with 200 μL of freshly prepared Griess reagent (1% sulfanilamide + 1% *n*-1-naphthyl-ethylenediamine hydrochloride 2.5% H_3PO_4) in a microwell plate and incubated for 30 min at 25 °C. The purple azo-dye generated after the reaction was measured at 540 nm.

2.10. Antioxidant assays

Based on the intracellular free-radical forming mechanisms, a total of multiple *in vitro* free radical scavenging assays (*i.e.*, hydroxyl radical, $OH^{\bullet}$; superoxide radical, $O_2^{\bullet -}$; singlet oxygen, $^1O_2$; hypochlorous acid, HOCl; hydrogen peroxide, H_2O_2; nitric oxide, NO; peroxynitrite, $OONO^-$) were selected to assess the overall antioxidant activities of the spice samples.[40] The reducing potential of the spices as a surrogate indicator of the general antioxidant activity was measured using a 2,2-diphenyl-1-picrylhydrazyl (DPPH) assay. Since transition metals can accelerate the intracellular free-radical formation cascade by potentiating the Fenton reaction, iron-chelation activity was measured, and to evaluate the potentials of the spices to limit free-radical mediated peroxidation of the cellular lipid, a lipid peroxidation assay was performed using chicken brain samples obtained from a local slaughterhouse. All assays were performed against appropriate standards as per our previously standardized methods adapted to a reduced volume suitable for microplates.[41,42] The range of the highest sample dose for each assay was based on the linear response range for the respective standard compounds in the final volume of the reaction mixture.

2.11. Statistical analysis

All data are reported as mean ± SEM of three replicates. Group comparisons were done by one-way ANOVA with Tukey's *post hoc* test using GraphPad V9. The percentage of inhibition/scavenging was calculated by the formula $[(X_0 - X_1)/X_0] \times 100$, where, X_0 is the absorbance of the control, and X_1 is the

absorbance in the presence of the samples and control. Linear correlation between independent variables was performed using Pearson's method. Data having unequal variances were log-transformed to achieve equal variances. Enrichment analysis was performed using MetaboAnalyst V5. The enrichment ratio for metabolites and pathways was calculated based on observed hit/expected hit values. Holm–Bonferroni correction for *p*-value and false discovery rate (FDR) was calculated for all entries of enrichment analysis. Pathway analysis was performed using Fisher's exact test. $p < 0.05$ was considered significant for all cases.

3. Results

3.1. MTT cytotoxicity

The treatment doses of LPS and FFA were selected based on an MTT cytotoxicity assay. Data showed that compared to untreated control cells, significant cell death occurred at 400 ng mL^{-1} LPS and 800 μM concentrations of FFA (Fig. 1A and B). The EC_{50} was calculated to be 747.75 ng mL^{-1} LPS and 1191.68 μM FFA. Therefore, a sublethal dose of 200 ng mL^{-1} for LPS and 400 μM concentration of FFA was selected for subsequent studies. However, it is noteworthy that lipid accumulation could affect the intracellular redox status that likely influenced the cytotoxicity assay outcomes. Indeed, the gross microscopic features of the treated cells indicate relatively increased steatotic bodies in FFA-treated cells compared to that of LPS, indicating increased intracellular lipid accumulation compared to LPS-treated cells (Fig. 1C and D).

3.2. Metabolomic profiling

The alteration of the intracellular metabolome was investigated using GC-MS analysis after appropriate derivatization. We identified (Fig. 2A–C and Tables S1–S3, ESI†) a total of 111, 65 and 85 metabolites in the control, LPS and FFA. The top 5 highly abundant metabolites in the control were D-(−)-lactic acid, (45.3%), oleic acid (8.8%), β-D-glucopyranose (5.9%), ethyl iso-allocholate (4.9%), and L-leucine (3.6%). The predominant metabolites in LPS were propanoic acid (11.3%), β-D-glucopyranose (8.8%), lactic acid (8.6%), D-(+)-mannopyranose (6.4%) and *trans*-9-octadecenoic acid (4.85), while D-lactic acid (66.2%), sebacic acid (6.8%), oleic acid (4.8%), azelaic acid (2.9%) and hexadecanoic acid (2.1%) were the most abundant metabolites in FFA. A total of 73, 32 and 53 unique metabolites were identified in the control, LPS and FFA (Fig. 2D). A total of 16 metabolites were common in all the treatments. Commonly unique metabolites in the control and LPS were 11, control and FFA were 11, and FFA and LPS were 4. The correlation heatmap depicted close association between the abundance of various metabolites with specific treatments (Fig. 2E). In particular, the overall association pattern was comparable between control and LPS, as reflected by the dendrogram. Chemical sub-class analysis revealed most significant abundance of saturated fatty acids and amino acids in all the treatments (Fig. 3A–C and

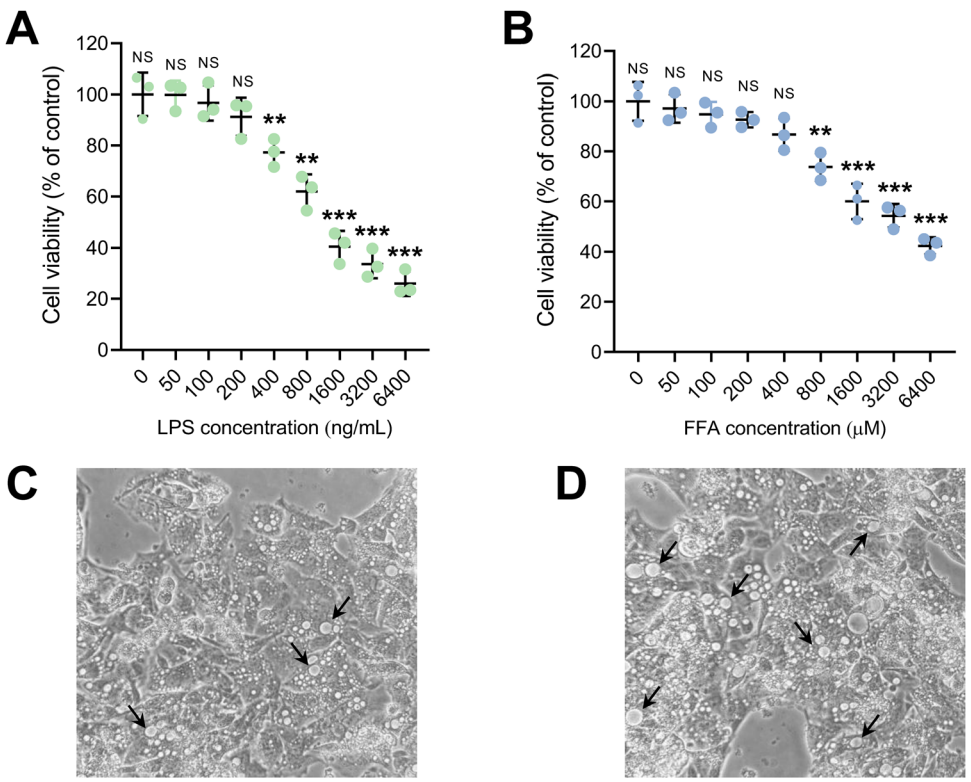

Fig. 1 Treatment effects on cell viability, lipid accumulation and inflammation. Effects of (A) LPS (0–800 ng mL^{-1}) and (B) FFA (0–1.6 mM) on the viability of HepG2 cells (24-h) measured by the MTT method. Visual representation of lipid accumulation (steatotic bodies) due to (C) LPS (200 ng mL^{-1}) and (D) FFA (400 μM) treatments of HepG2 cells. Abbreviations: LPS, lipopolysaccharide; FFA, free fatty acid (palmitate).

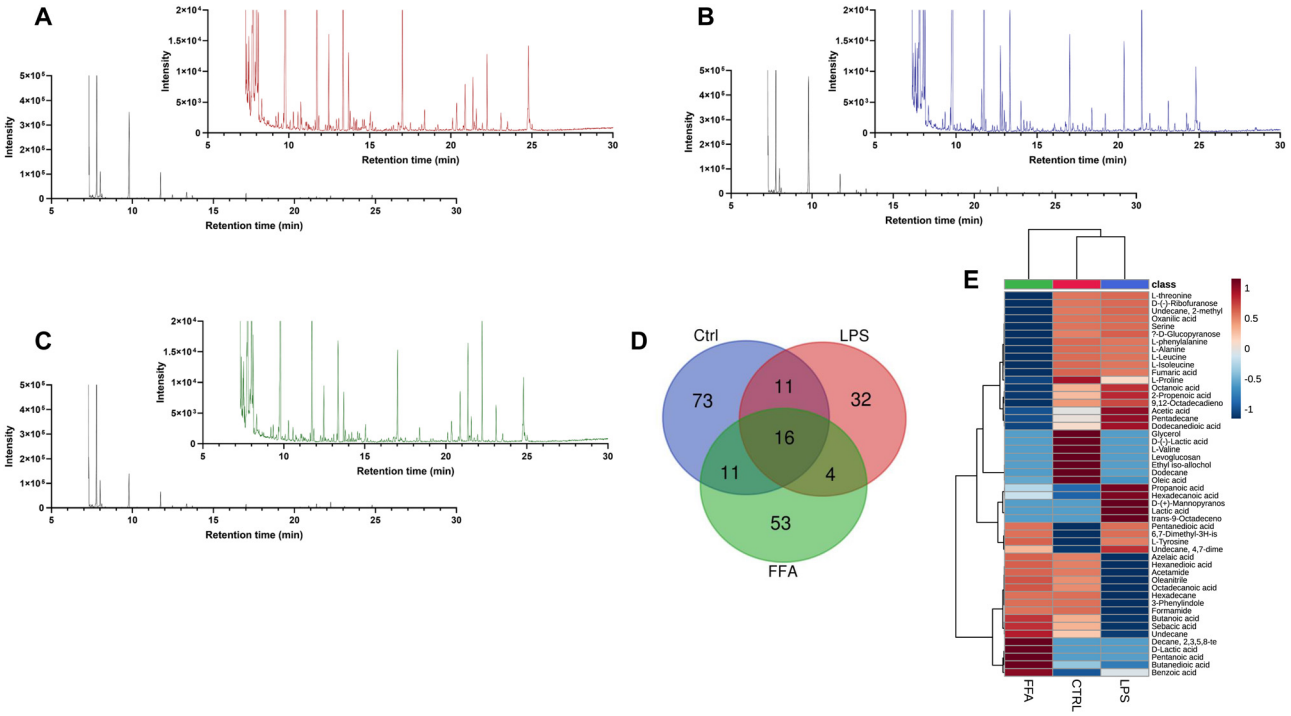

Fig. 2 Gas chromatography-mass spectrometry (GCMS) analysis of the cell-free metabolites. (A) Control, (B) LPS, and (C) FFA. A list of identified metabolites is provided in the ESI,† Tables S1–S3. (D) Vein diagram depicting common metabolites. (E) Heatmap depicting the association of the metabolite abundance with various treatments. Abbreviations: Ctrl, control; LPS, lipopolysaccharide; FFA, free fatty acid (palmitate).

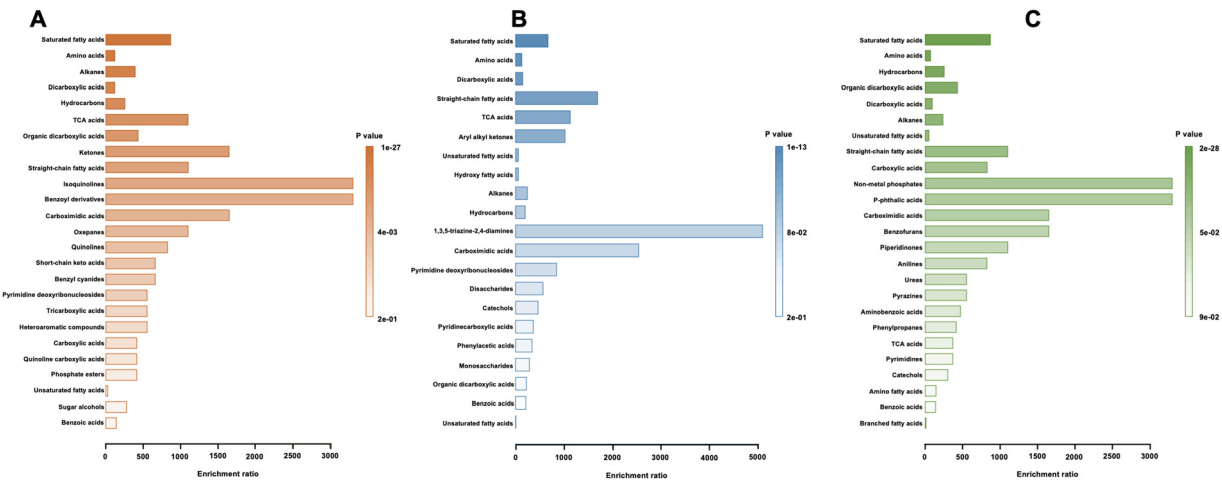

Fig. 3 Metabolite enrichment analysis of (A) Ctrl, (B) LPS, and (C) FFA at a sub-class of chemicals (data corresponds to Tables S4–S6, ESI†). Enrichment ratio was calculated by observed metabolite hits/expected hits. Abbreviations: Ctrl, control; LPS, lipopolysaccharide; FFA, free fatty acid (palmitate).

Tables S4–S6, ESI†). However, isoquinone and benzyl derivatives in the control, 1,3,5-triazine-2,4-diamines and carboximidic acids in LPS (Fig. 3B), and non-metal phosphates and *p*-phthalic acids were the highly enriched chemical classes in FFA (Fig. 3C).

3.3. Enrichment and pathway analysis

The identified metabolites were mapped against respective biosynthetic pathways based on the small molecule pathway database. Data showed that fatty acid biosynthesis; valine, leucine and isoleucine degradation, alanine metabolism, arginine and proline metabolism, and glutathione metabolism were the top five most significantly enriched metabolic pathways in the control (Fig. 4A and Table S7, ESI†). The patterns of pathway enrichment were altered under LPS and FFA treatment. Phenylalanine and tyrosine metabolism, trehalose degradation, the Warburg effect, fatty acid biosynthesis, and the mitochondrial electron transport chain in LPS (Fig. 4B and Table S8, ESI†), whereas urea cycle,

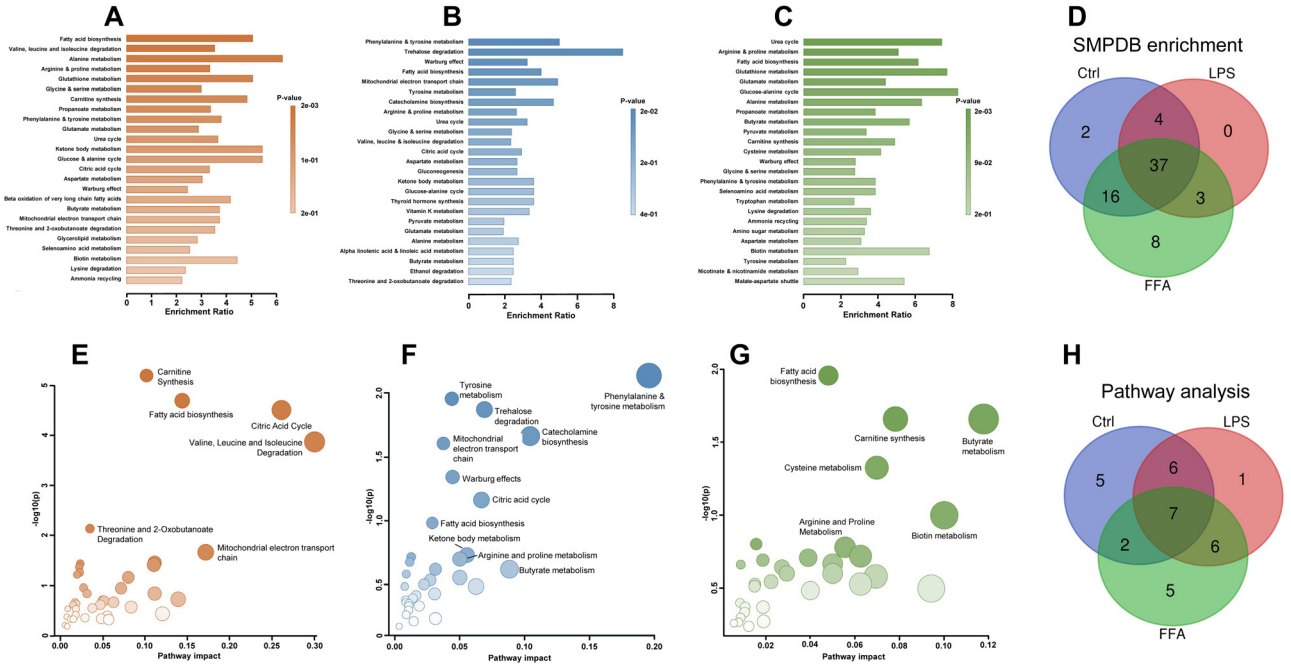

Fig. 4 Treatment effects on intracellular metabolic pathways. Pathway enrichment in control (A), LPS (B), and (C) FFA-treated cells (data corresponds to Tables S7–S9, ESI†). Venn diagram depicting commonly enriched pathways (D). log normalized pathway impacts in control (E), LPS (F), and (G) FFA-treated cells (data corresponds to Tables S10–S12, ESI†). Venn diagram depicting commonly impacted pathways (H).

arginine and proline metabolism, fatty acid biosynthesis, glutathione metabolism, and glutamate metabolism were the top five enriched pathways in FFA (Fig. 4C and Table S9, ESI†). Among these, only 4 pathway enrichments were common between control and LPS, whereas 16 were common between control and FFA (Fig. 4D). Homocysteine degradation and porphyrin metabolism in the control, and glycerol phosphate shuttle, inositol metabolism, D-arginine and D-ornithine metabolism, inositol phosphate metabolism, spermidine and spermine biosynthesis, betaine metabolism, lactose synthesis and vitamin B6 metabolism were uniquely identified in FFA. Furthermore, pathway impact analysis revealed that in the control (Fig. 4E and Table S10, ESI†), the top five most significantly impacted pathways were carnitine synthesis, fatty acid biosynthesis, citric acid cycle, valine, leucine and isoleucine degradation, and threonine and 2-oxobutanoate degradation pathways. In LPS (Fig. 4F and Table S11, ESI†), the top five impacted pathways were phenylalanine and tyrosine metabolism, tyrosine metabolism, trehalose degradation, catecholamine biosynthesis, and mitochondrial electron transport chain; whereas the same in the FAA group (Fig. 4G and Table S12, ESI†) were fatty acid biosynthesis, butyrate metabolism, carnitine synthesis, cysteine metabolism, and biotin metabolism. Only plasmalogen synthesis was unique in the LPS group whereas mitochondrial beta-oxidation of long chain saturated fatty acids, sulfate/sulfite metabolism, lysine degradation, mitochondrial beta-oxidation of short chain saturated fatty acids, and cysteine metabolism were unique pathways in FFA (Fig. 4H).

3.4. Gene expression

LPS and FFA differentially influenced the gene expressions in HepG2 cells (Fig. 5). The mRNA expression of TLR4 and MyD88

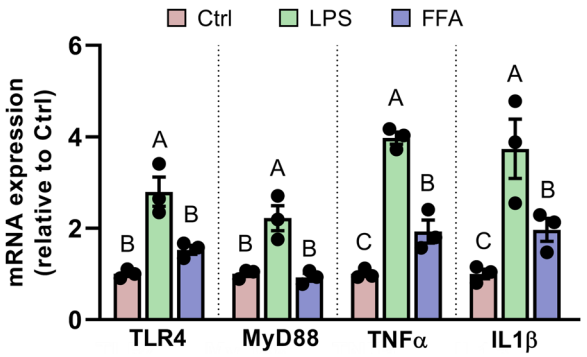

Fig. 5 mRNA expressions of inflammatory parameters. Data represented as mean ± SEM of 3 replicates. Abbreviations: LPS, lipopolysaccharide; FFA, free fatty acid (palmitate); Ctrl, control; TLR4, Toll-like receptor 4; MyD88, myeloid differentiation primary response 88; TNFα, tumor necrosis factor α; IL1β, interleukin 1β.

were significantly increased due to LPS treatment at 2.2–2.8-times. LPS also resulted in 3.9–3.7-times increased mRNA expression of TNFα and IL1β. Compared to the control, FFA had no significant impact on the mRNA expression of TLR4 and MyD88, although TLR4 was increased 1.5-times. The expression of both TNFα and IL1β was significantly increased 1.9-times compared to the control; however, they were 45–58% lower compared to LPS.

3.5. Antioxidant enzymes

The effects of LPS and FAA on the cytoprotective enzymes and oxidative stress were evaluated using biochemical assays.

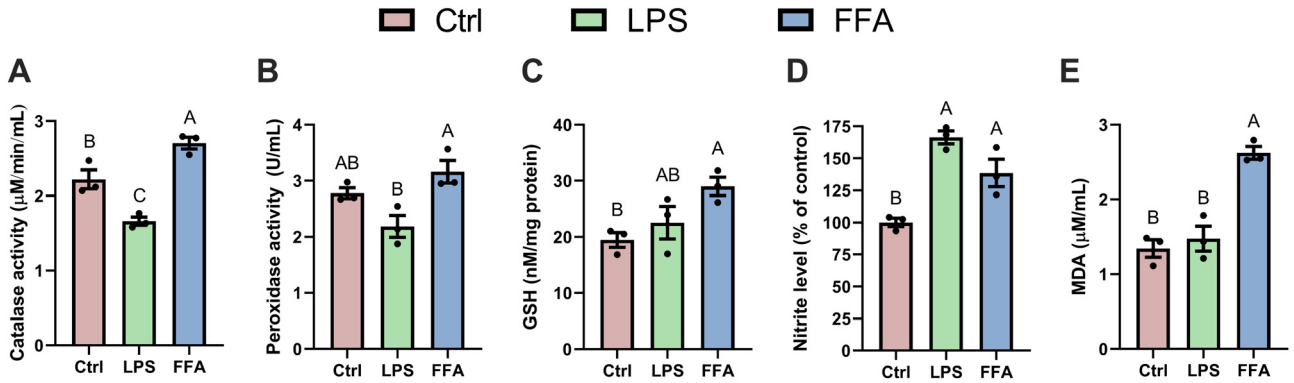

Fig. 6 Treatment effects (24-h) on (A) catalase activity; (B) peroxidase activity; (C) GSH level; (D) nitrite level; (E) MDA level. Data represented as mean ± SEM of 3 replicates. Abbreviations: Ctrl, control; LPS, lipopolysaccharide; FFA, free fatty acid (palmitate); GSH, glutathione; NO, nitric oxide; MDA, malondialdehyde.

Data showed that compared to the control, LPS-treatment reduced (24.8%) the cellular catalase activity whereas it was elevated (1.2-times) due to FAA (Fig. 6A). The peroxidase activity was lowered (21.3%; $P = 0.11$) while FAA treatment increased (1.1-times) the peroxidase activity (Fig. 6B). While the GSH level was elevated both due to LPS (1.2-times) and FFA (1.5-times), the increase was significant only for FFA ($P = 0.03$) (Fig. 6C). Both LPS (1.6-times) and FFA (1.4-times) elevated the nitrite release compared to the control (Fig. 6D). Finally, only FFA significantly increased (1.9-times; $P = 0.001$) the lipid peroxidation compared to the control (Fig. 6E). It is noteworthy that a significant increase of catalase (1.68-times; $P = 0.001$), peroxidase (1.44-times; $P = 0.016$), and MDA (1.87-times; $P = 0.001$) levels was observed due to FFA treatment compared to LPS. Compared to LPS, the level of GSH was increased (1.3-times; $P = 0.14$) while nitrite was decreased (16.7%; $P = 0.07$), but not to the level of significance.

3.6. *In vitro* antioxidant assay

Beyond the intracellular cytoprotective enzymes, intracellular metabolites are known to limit cellular oxidative damage by directly scavenging the free radicals. Thus, the free-radical scavenging potentials of the cell-free metabolites were measured using biochemical assays relevant to the intracellular cascade of free-radical formation (Fig. 7A). Data showed that (Fig. 7B) control metabolites were overall better scavengers of free radicals compared to LPS and FFA metabolites. For the DPPH assay, the CTRL was ~1.85-times better ($p = 0.04$) compared to both LPS and FFA. Compared to the control, the hydroxyl scavenging capacities of LPS (85.3%; $p = 0.001$) and FFA (49.8%; $p = 0.01$) were lower compared to the control. The superoxide scavenging potential of the control was 1.84 to 2-times better ($p = 0.05$) than both treatments. LPS metabolites demonstrated 60.7% ($p = 0.01$) lower H_2O_2 scavenging potential than the control, while the same was 25.6% lower for FFA ($p = 0.05$). For nitric oxide scavenging, the control demonstrated better capacity compared to LPS (2-times; $p = 0.012$) and FFA (1.35-times; $p = 0.139$). In the case of peroxynitrite scavenging, LPS (35.1%; $p = 0.28$) and FFA (73.6%; $p = 0.029$) demonstrated lower activities compared to the control. In the case of iron chelation potential, the control demonstrated better activities compared to LPS (2.5-times; $p = 0.041$) and FFA (1.44-times; $p = 0.30$). Finally, both LPS (46.8%; $p = 0.01$) and FFA (18.54%; $p = 0.05$) showed lower lipid peroxidation inhibitory activities than the control. For most all bioactivities, LPS and FFA demonstrated statistically comparable bioactivities except for hydroxyl radicals and H_2O_2 scavenging and lipid peroxidation inhibitory potential. For these activities, FFA demonstrated 3.43, 1.89, and 1.53-times higher bioactivities relative to LPS.

4. Discussion

The current study presented a comparative account of the differential effects of sub-lethal dose of endotoxin and albumin-conjugated FFA on liver injury. Although endotoxemia and lipotoxicity are known to occur simultaneously during the course of the MASLD spectrum, a comparative effect of the individual injuries on liver cells in terms of changes in the intracellular metabolome remained unknown. We demonstrated that both LPS and FFA treatment of HepG2 cells induced inflammation, but unlike LPS, FFA had no effects on TLR4/MyD88 mRNA expression. LPS reduced intracellular antioxidant defense but no changes in lipid peroxidation were observed. Whereas, FFA-treatment induced lipid peroxidation and elevated the levels of antioxidant enzymes. Cell-free metabolites of LPS-treated cells demonstrated lower free-radical scavenging potentials compared to that of FFA-treated cells. Finally, both treatments revealed distinct, yet overlapping intracellular metabolomic features that helped to decipher altered intracellular metabolic pathways under the influence of both treatments.

Among the intracellular metabolites identified, lactic acid was predominant in both the treatments. Indeed, high abundance of lactic acid was reported in the serum of MASLD patients,[43] and hyperacetylation of the lactate dehydrogenase enzyme is seen in the liver of MASLD patients, resulting in hepatic lactate accumulation.[44] Abundance of oleic acid under LPS and FFA-treatment was comparatively lower compared to

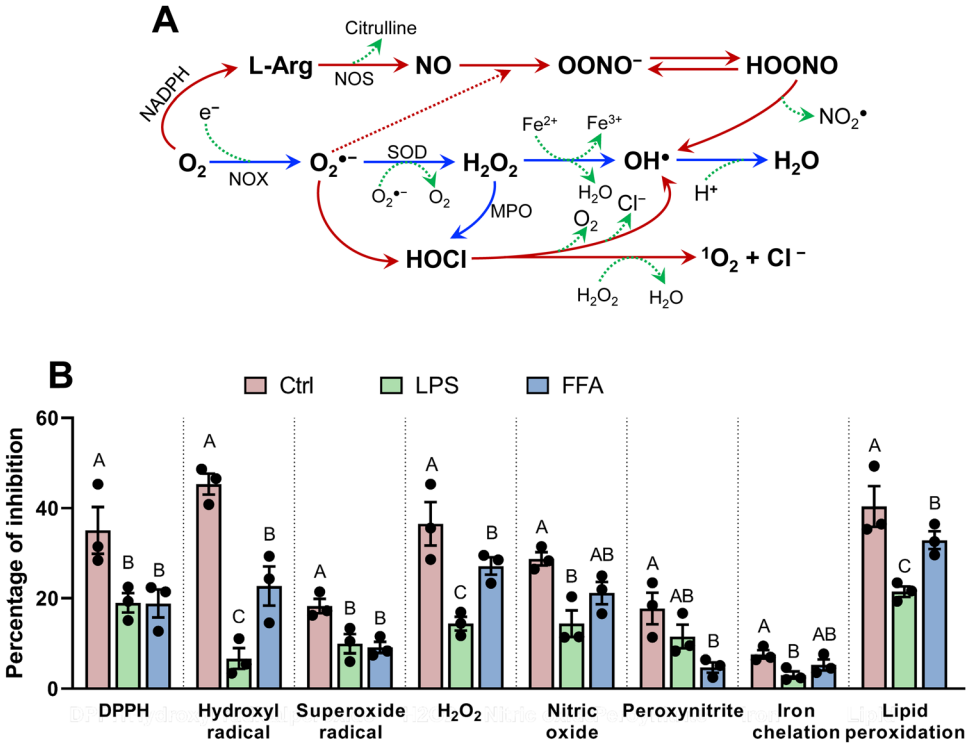

Fig. 7 Effects of cell-free metabolites on free-radical scavenging activities. (A) Intracellular free-radical formation cascade. The major reactive oxygen and nitrogen species were studied. (B) Free-radical scavenging effects of the cell-free sample. Metabolites of Ctrl, LPS and FFA-treated (24-h) cells. Data represented as mean ± SEM of 3 replicates. Abbreviations: Ctrl, control; LPS, lipopolysaccharide; FFA, free fatty acid (palmitate); L-arg, L-arginine, NO, nitric oxide; NOX, NADPH oxidase; O_2, superoxide radical; SOD, superoxide dismutase; H_2O_2, hydrogen peroxide; $OH^•$, hydroxyl radical; MPO, myeloperoxidase; HOCl, hypochlorous acid; $^1O_2$, singlet oxygen; HOCl, hypochlorous acid; $OONO^-$, peroxynitrite anion; HOONO; peroxynitrous acid; NO_2, nitrogen dioxide radical.

untreated control cells. Although similar to the FFA (palmitate) in the current study, oleic acid is also used to mimic MASLD *in vitro*, recent experimental evidence suggests that oleic acid can ameliorate palmitate-induced lipotoxicity in HepG2 cells by endoplasmic reticulum stress and inflammatory cell death.[45] Cholic acid methyl ester (ethyl iso-alcoholate) was highly abundant in the control, but absent in LPS and FFA-treated cells. According to earlier studies, ethyl iso-alcoholate not only limits liver metastasis,[45] but cholic acid derivatives have been reported to be associated with the regulation of several normal hepatic functions including inflammatory response, oxidative damage, energy metabolism and detoxification.[46,47] Sebacic acid, a saturated dicarboxylic acid, was only enriched in FFA-treated cells, and is also predominantly present in the circulation of MASLD patients.[48] We identified the highest enrichment of propanoic acid in LPS-treated cells, which is contradictory to earlier studies demonstrating its beneficial effects on the liver *in vivo*.[49] Nevertheless, others have reported propanoic acid treatment-associated oxidative damage in rat liver.[50] Among the specific chemical sub-class enrichments, saturated fatty acids were most highly enriched under both the treatments. Indeed, saturated fatty acids are lipidomic markers of MASLD,[51] where hepatocellular lipid accumulation and endoplasmic reticulum stress are all caused by the rise in saturated fatty acids in the hepatocytes.[51]

The identified metabolites were further mapped against SMPDB to decipher the treatment effects against intracellular metabolic and biochemical pathways. Several identified highly enriched metabolic pathways showed association with the treatment effects. For instance, the data showed that metabolic pathways pertaining to phenylalanine and tyrosine metabolism were highly enriched under LPS treatment. Indeed, this is supported by earlier studies reporting that treatment of experimental mice with LPS-rich Gram negative bacteria influences hepatic steatosis by impacting phenylalanine metabolism, while supplementation of mice with phenylalanine aggravates hepatic injury.[52] In fact, the hydroxylation process through which phenylalanine is converted to tyrosine predominantly takes place in the liver, which is elevated in chronic inflammatory liver conditions such as advanced cirrhosis.[53] We also identified the Warburg effect predominant in LPS-treated cells, which is adaptation of cells from citric acid cycle and oxidative phosphorylation to glycolysis and lactic acid fermentation for the generation of energy. Earlier studies indeed reported the Warburg effect in MASLD,[54] and that increased lactate production and lack of clearance can promote lipogenic gene expression, increased intracellular lipid uptake and steatosis in MASLD.[44] In fact, metabolic reprogramming of inflammatory cells under several chronic inflammatory diseases is closely associated with the shift in metabolism away from oxidative

phosphorylation towards aerobic glycolysis.[55] Indeed, enrichment of glycolysis was identified as the only uniquely enriched pathway in LPS-treated cells. In FFA-treated cells, the urea cycle was highly impacted based on the metabolite mapping. Studies *in vivo* report that hypermethylation of urea cycle-associated genes and impairment of urea synthesis is a hallmark of MASLD, where hepatocellular fat accumulation irreversibly diminishes hepatic ammonia detoxification.[56] Reduced hepatic ammonia is associated with the formation of L-ornithine (later converts into L-proline) and urea from L-arginine. Indeed, pathway enrichment data showed that arginine and proline metabolism were enriched in cells with FFA. This was supported by an earlier *in vivo* study demonstrating dysfunctional arginine and proline metabolism in experimental mice with MASLD.[57] Interestingly, compared to LPS, GSH metabolism was highly enriched in FFA-treated cells, indicating increased oxidative stress in response to FFA. Significantly elevated GSH level is not only observed in the present study, but supportive data from an earlier comparable study with fatty acid overload in HelG2 cells reported positive association between hepatocellular steatosis and GSH level.[58]

In terms of inflammatory injury, LPS treatment demonstrated comparatively higher inflammation than FFA. This is evident by the higher mRNA expression of TNFα and IL1β in LPS-treated cells compared to that of FFA. Although FFA also increased the levels of the pro-inflammatory mediators, these increases were independent from stimulation of TLR4/MyD88 signaling, which was otherwise significantly elevated due to LPS treatment. Gut-derived LPS translocation along the portal vein is known to trigger hepatic inflammation by activating the TLR4/MyD88-signaling. Indeed, increased serum endotoxin is a marker for MASLD and metabolic endotoxemia that is associated with hepatic inflammation.[8] Earlier studies report that saturated fatty acids can also activate TLR4 signaling,[59] and that lipid-induced inflammation is predominantly mediated by TLR4 signaling.[60] However, no significant increase of TLR4 and MyD88 mRNA expression was observed associated with the increased expression of TNFα and IL1β under the influence of FFA. Indeed, these observations are consistent with recent data showing that saturated FA palmitate does not function as a TLR4 agonist.[61] Contrarily, others have reported that palmitate can trigger NFκB-dependent metainflammation in adipose and skeletal muscle cells *in vitro*.[62,63] An alternative inflammatory mechanism of FFA could be the activation of the transcription factor signal transducer and activator of transcription-3 (STAT3), which is triggered in the liver during the course of progressive liver metabolic disease.[64] Additionally, a TLR2/STAT3-dependent inflammatory cascade has been attributed to inflammatory insults during MASLD.[65] Nevertheless, several contrary studies *in vitro* and *in vivo* show that unsaturated fatty acids can inhibit STAT3-associated cellular responses in HepG2[66] and other cells.[67,68] Our data also show that compared to LPS, FFA exerts lower inflammatory insults on HepG2 cells. Although there is no previous literature available comparing endotoxin and FA in terms of hepatic inflammation, it is likely that FFA-mediated inflammation, moderate relative to LPS, results due to intracellular oxidative damage. Indeed, oxidative stress-induced inflammation is well-established in MASLD.[69,70] In support, experimental evidence shows that treatment of HepG2 cells with antioxidant *n*-acetylcysteine reduces inflammatory damage,[71] whereas suppression of hepatocellular cytoprotective transcription factors can induce inflammation.[72] Further investigation is warranted along these lines of research.

We also investigated the individual effects of LPS and FFA on the intracellular oxidative stress response. Data showed relatively lower catalase and peroxidase levels due to LPS treatment, while the same parameters were increased due to FFA compared to controls. It is known that the enzymatic levels and the activities of both the enzymes are tightly regulated by the extent of intracellular oxidative stress.[73,74] Earlier studies report that LPS treatment can lower the activities of intracellular cytoprotective enzymes in a dose-dependent manner, while elevating the levels of pro-inflammatory IL6, IL1β and TNFα in parallel[75] and that LPS-treatment lowers the intracellular oxidative stress-response in hepatic endothelial and Kupffer cells.[76] Indeed, others have shown that chemical-induced deactivation of cellular antioxidant enzymes can exacerbate LPS-induced liver damage.[77] FAA on the other hand increased the level of catalase, peroxidase and GSH, and these data are supported by earlier studies demonstrating that palmitate triggers the increase of intracellular antioxidative enzymes in response to oxidative stress.[78]

Although the cytoprotective enzymes are transcriptionally regulated by common factors (*e.g.*, Nrf2, FOXO, *etc.*), each enzyme is tightly regulated by specific combinations of intracellular responses and is associated with different functions. For instance, data suggest that catalase activity plays a pivotal role against oxidative stress-induced cell damage compared to GSH.[79] Our data showed the relatively opposite trend for the antioxidant enzymes for both the treatments. Although out of the scope of the study, it is likely that LPS-associated inflammation could degrade and lower the intracellular enzymatic activities, where the higher enzymatic activities under FFA were due to the increase in intracellular oxidative stress response. Indeed, data from patients with metabolic syndrome show an inverse association between the levels of antioxidant enzymes and inflammatory markers.[80] Cellular data also show that LPS-treatment of HepG2 cells is associated with lower activities of antioxidant enzymes.[81] Furthermore, the level of soluble NO was increased due to both treatments, with LPS causing a greater increase relative to FFA. This is supported by the fact that LPS-induced activation of TLR4/MyD88-signaling results in activation of iNOS and release of NO in various experimental models.[82,83] Additionally, the effects of LPS and FFA on cellular oxidative stress were demonstrated by the level of lipid peroxidation where only FFA treatment resulted in increased MDA level, demonstrating significant oxidative injury to HepG2 cells due to FFA.

Based on recent reports that the intracellular metabolome is a better predictor of cellular behavior under pathophysiological injury[84] and that the cellular metabolome could be a suitable marker of disease pathogenesis,[85] we intended to investigate the targeted free-radical scavenging activities of the cell-free metabolites of HepG2 cells with or without the treatments. For

this purpose, assay-specific reactions were set based on *in vitro* production of specific free radicals dedicated for specific purposes.[86] Overall, a striking impact of the metabolites was observed in the case of the components of the Fenton reaction and that of the Haber–Weiss reaction. Generally, intracellular formation of the highly reactive $OH^{\bullet}$ is dependent on H_2O_2 alone or due to the reaction between H_2O_2 and $O_2^{\bullet -}$.[40] In both instances, transition metal Fe^{2+} plays an important role as a catalyst. Our data show that cell-free metabolites of FFA relative to LPS, holds better potential in inhibiting $OH^{\bullet}$ and H_2O_2; however, comparable activities of both were noted in the case of $O_2^{\bullet -}$ scavenging and Fe^{2+} chelation. Although the bioactivities of the cell-free metabolites of LPS and FFA were statistically comparable for most cases, FFA demonstrated significantly higher lipid peroxidation inhibitory effects than LPS, indicating better cellular protection by FFA than LPS. It is noteworthy that under this experimental design, the observed antioxidant effects cannot be attributed to any specific metabolite but rather are the result of the additive and cumulative effects of the entire metabolome. Specific metabolites identified are already known to exert cytoprotective effects. For instance, an earlier study reports that proline can effectively reduce ROS and improve cell survival against oxidative stress by increasing intracellular levels through the overexpression of biosynthetic enzymes.[87] Conversely, cellular manipulations that deplete proline levels reduce cell survival, which additional antioxidants can counteract. Others report that valine has a significant protective role against mitochondrial ROS and cellular damage because it improves mitochondrial biogenesis and dynamics, influences electron transport chain complexes, lowers mitochondrial reactive oxygen species, and increases ATP generation during oxidative stress.[88] Despite this evidence, since we tested the cytoprotective effects using the cellular metabolome, identifying the main bioactive metabolite remains out of the scope of the current study.

5. Conclusion

Initiation and progression of the MASLD-spectrum of diseases are associated with inflammatory injury due to gut-derived endotoxin, and steatosis due to adipose-derive lipotoxicity. In obese individuals with metabolic syndrome, both injuries are known to occur simultaneously. The current study intended to decipher the intracellular metabolomic changes that are exclusive to endotoxemia and lipotoxicity. Data showed that although both treatments triggered inflammation, FFA induced greater oxidative injury to HepG2 cells compared to LPS. The cell-free metabolites of LPS and FFA-treated cells demonstrated comparable activities in scavenging of free-radicals. Finally, untargeted metabolomics analysis revealed enrichments of distinct sets of metabolic pathways due to LPS and FFA. It is noteworthy that beyond GCMS-based metabolomics, additional utilization of LCMS-based approaches would likely result in the identification of diverse classes of metabolites, which remains to be explored in future studies. Nevertheless, the current study provided a GCMS-based overview of the altered intracellular metabolome due to endotoxemia and lipotoxic injury, and could lead to the understanding of hepatocellular behavior through future translational studies.

Author contributions

JS and PD performed the experiments; PD wrote the manuscript. Both authors have read and approved the final copy of the manuscript.

Data availability

All raw data of the study are available in the ESI† and can be retrieved from Metabolomics Workbench. Link: **https://dev.metabolomicsworkbench.org:22222/data/DRCCMetadata.php?Mode=Study&StudyID=ST003475&Access=IyqT5950**. The DOI for this project (PR002134) is: **https://dx.doi.org/10.21228/M8S53W**.

Conflicts of interest

The authors declare no conflict of interest.

Acknowledgements

Funding received from the Science and Engineering Research Board (SRG/2021/000082) is thankfully acknowledged. The authors are thankful to Dr Monisha Dhiman, Department of Microbiology. Central University of Punjab, for helping with the GC-MS analysis.

References

1 A. Soto, C. Spongberg, A. Martinino and F. Giovinazzo, *Biomedicines*, 2024, **12**, 397.
2 W.-K. Chan, K.-H. Chuah, R. B. Rajaram, L.-L. Lim, J. Ratnasingam and S. R. Vethakkan, *J. Obes. Metab. Syndr.*, 2023, **32**, 197.
3 S. Pouwels, N. Sakran, Y. Graham, A. Leal, T. Pintar, W. Yang, R. Kassir, R. Singhal, K. Mahawar and D. Ramnarain, *BMC Endocr. Disord.*, 2022, **22**, 1–9.
4 J. M. Kneeman, J. Misdraji and K. E. Corey, *Ther. Adv. Gastroenterol.*, 2012, **5**, 199–207.
5 M. Branković, I. Jovanović, M. Dukić, T. Radonjić, S. Oprić, S. Klašnja and M. Zdravković, *Int. J. Mol. Sci.*, 2022, **23**, 23147894.
6 T. Kessoku, T. Kobayashi, K. Imajo, K. Tanaka, A. Yamamoto, K. Takahashi, Y. Kasai, A. Ozaki, M. Iwaki, A. Nogami, Y. Honda, Y. Ogawa, S. Kato, T. Higurashi, K. Hosono, M. Yoneda, T. Okamoto, H. Usuda, K. Wada, N. Kobayashi, S. Saito and A. Nakajima, *Front. Endocrinol.*, 2021, **12**, 770986.
7 P. Dey, *Pharmacol. Res.*, 2020, **161**, 105135.
8 A. L. Harte, N. F. da Silva, S. J. Creely, K. C. McGee, T. Billyard, E. M. Youssef-Elabd, G. Tripathi, E. Ashour,

M. S. Abdalla, H. M. Sharada, A. I. Amin, A. D. Burt, S. Kumar, C. P. Day and P. G. McTernan, *J. Inflammation*, 2010, **7**, 15.

9 J. Soppert, E. F. Brandt, N. M. Heussen, E. Barzakova, L. M. Blank, L. Kuepfer, M. W. Hornef, J. Trebicka, J. Jankowski and M.-L. Berres, *Clin. Gastroenterol. Hepatol.*, 2022, **21**, 2746–2758.

10 P. Dey, B. D. Olmstead, G. Y. Sasaki, Y. Vodovotz, Z. Yu and R. S. Bruno, *J. Nutr. Biochem.*, 2020, **84**, 108455.

11 T. Csak, A. Velayudham, I. Hritz, J. Petrasek, I. Levin, D. Lippai, D. Catalano, P. Mandrekar, A. Dolganiuc and E. Kurt-Jones, *Am. J. Physiol.: Gastrointest. Liver Physiol.*, 2011, **300**, G433–G441.

12 Y. Geng, K. N. Faber, V. E. de Meijer, H. Blokzijl and H. Moshage, *Hepatol. Int.*, 2021, **15**, 21–35.

13 Z. Zhu, X. Zhang, Q. Pan, L. Zhang and J. Chai, *Liver Res.*, 2023, **7**, 285–295.

14 L. Zu, J. He, H. Jiang, C. Xu, S. Pu and G. Xu, *J. Biol. Chem.*, 2009, **284**, 5915–5926.

15 R. Parker, *Liver Res.*, 2018, **2**, 35–42.

16 F. B. Lu, K. I. Zheng, R. S. Rios, G. Targher, C. D. Byrne and M. H. Zheng, *J. Gastroenterol. Hepatol.*, 2020, **35**, 2041–2050.

17 R. Xu, J. Pan, W. Zhou, G. Ji and Y. Dang, *Biomed. Pharmacother.*, 2022, **153**, 113331.

18 G. N. Ioannou, G. A. Nagana Gowda, D. Djukovic and D. Raftery, *Metabolites*, 2020, **10**, 168.

19 H. J. Yoo, K. J. Jung, M. Kim, M. Kim, M. Kang, S. H. Jee, Y. Choi and J. H. Lee, *Front. Physiol.*, 2019, **10**, 1421.

20 Q. Huang, Y. Tan, P. Yin, G. Ye, P. Gao, X. Lu, H. Wang and G. Xu, *Cancer Res.*, 2013, **73**, 4992–5002.

21 A. J. McGlinchey, O. Govaere, D. Geng, V. Ratziu, M. Allison, J. Bousier, S. Petta, C. de Oliviera, E. Bugianesi and J. M. Schattenberg, *JHEP Rep.*, 2022, **4**, 100477.

22 N. Kano, E. J. Want and M. J. McPhail, *Curr. Treat. Options Gastroenterol.*, 2021, **19**, 380–397.

23 R. Ganesan, S. J. Yoon and K. T. Suk, *Int. J. Mol. Sci.*, 2022, **24**, 537.

24 N. Adil, A. J. Siddiqui and S. G. Musharraf, *Scand. J. Immunol.*, 2022, **96**, e13208.

25 G. Raja, H. Gupta, Y. A. Gebru, G. S. Youn, Y. R. Choi, H. S. Kim, S. J. Yoon, D. J. Kim, T.-J. Kim and K. T. Suk, *Int. J. Mol. Sci.*, 2021, **22**, 1160.

26 S. P. Cousin, S. R. Hügl, C. E. Wrede, H. Kajio, M. G. Myers Jr and C. J. Rhodes, *Endocrinology*, 2001, **142**, 229–240.

27 I. T. de Almeida, H. Cortez-Pinto, G. Fidalgo, D. Rodrigues and M. E. Camilo, *Clin. Nutr.*, 2002, **21**, 219–223.

28 H. Malhi, S. F. Bronk, N. W. Werneburg and G. J. Gores, *J. Biol. Chem.*, 2006, **281**, 12093–12101.

29 E. Karaskov, C. Scott, L. Zhang, T. Teodoro, M. Ravazzola and A. Volchuk, *Endocrinology*, 2006, **147**, 3398–3407.

30 A. F. Oliveira, D. A. Cunha, L. Ladriere, M. Igoillo-Esteve, M. Bugliani, P. Marchetti and M. Cnop, *Biotechniques*, 2015, **58**, 228–233.

31 R. Rezgui, R. Walia, J. Sharma, D. Sidhu, K. Alshagadali, S. Ray Chaudhuri, A. Saeed and P. Dey, *Antioxidants*, 2023, **12**, 930.

32 P. Dey and T. K. Chaudhuri, *Cytotechnology*, 2016, **68**, 749–761.

33 P. Dey, N. Tewari, S. Dutta, R. A. Newman and T. K. Chaudhuri, *J. Ethnopharmacol.*, 2024, **323**, 117717.

34 P. Dey and T. K. Chaudhuri, *J. Food Biochem.*, 2016, **40**, 630–635.

35 D. Sidhu, M. Vasundhara and P. Dey, *RSC Adv.*, 2024, **14**, 33034–33047.

36 S. Gandhi, M. R. Saha and P. Dey, *Heliyon*, 2023, **9**, e21392.

37 J. Li, G. Y. Sasaki, P. Dey, C. Chitchumroonchokchai, A. N. Labyk, J. D. McDonald, J. B. Kim and R. S. Bruno, *J. Nutr. Biochem.*, 2018, **53**, 58–65.

38 P. Dey, E. Mah, J. Li, T. Jalili, J. D. Symons and R. S. Bruno, *J. Funct. Foods*, 2018, **40**, 670–678.

39 M. R. Saha, P. Dey, I. Sarkar, D. De Sarker, B. Haldar, T. K. Chaudhuri and A. Sen, *J. Ethnopharmacol.*, 2018, **210**, 275–286.

40 S. Dutta, P. Dey, M. R. Saha, I. Sarkar, R. Sarkar, J. A. Mardi, J. Barman, A. Sen and T. K. Chaudhuri, *J. Funct. Foods*, 2017, **39**, 112–122.

41 M. R. Saha, P. Dey, S. Begum, B. De, T. K. Chaudhuri, D. D. Sarker, A. P. Das and A. Sen, *PLoS One*, 2016, **11**, e0150574.

42 M. R. Saha, P. Dey, T. K. Chaudhuri, A. K. Goyal, D. D. Sarker and A. Sen, *Indian J. Exp. Biol.*, 2016, **54**, 115–125.

43 H. E. Da Silva, A. Teterina, E. M. Comelli, A. Taibi, B. M. Arendt, S. E. Fischer, W. Lou and J. P. Allard, *Sci. Rep.*, 2018, **8**, 1466.

44 T. Wang, K. Chen, W. Yao, R. Zheng, Q. He, J. Xia, J. Li, Y. Shao, L. Zhang, L. Huang, L. Qin, M. Xu, Z. Zhang, D. Pan, Z. Li and F. Huang, *J. Hepatol.*, 2021, **74**, 1038–1052.

45 X. Zeng, M. Zhu, X. Liu, X. Chen, Y. Yuan, L. Li, J. Liu, Y. Lu, J. Cheng and Y. Chen, *Nutr. Metab.*, 2020, **17**, 1–14.

46 J. P. Arab, S. J. Karpen, P. A. Dawson, M. Arrese and M. Trauner, *Hepatology*, 2017, **65**, 350–362.

47 T.-Y. Jiao, Y.-D. Ma, X.-Z. Guo, Y.-F. Ye and C. Xie, *Acta Pharmacol. Sin.*, 2022, **43**, 1103–1119.

48 L. Liu, J. Zhao, R. Zhang, X. Wang, Y. Wang, Y. Chen and R. Feng, *J. Pharm. Biomed. Anal.*, 2021, **200**, 114058.

49 A. C. Tengeler, E. Gart, M. Wiesmann, I. A. Arnoldussen, W. van Duyvenvoorde, M. Hoogstad, P. J. Dederen, V. Verweij, B. Geenen and T. Kozicz, *FASEB J.*, 2020, **34**, 9575–9593.

50 S. Al-Daihan and R. Shafi Bhat, *Int. J. Mol. Cell. Med.*, 2015, **4**, 188–195.

51 S. Kartsoli, C. E. Kostara, V. Tsimihodimos, E. T. Bairaktari and D. K. Christodoulou, *World J. Hepatol.*, 2020, **12**, 436–450.

52 L. Chen, P. Yang, L. Hu, L. Yang, H. Chu and X. Hou, *Cell Biosci.*, 2023, **13**, 24.

53 P. Tessari, M. Vettore, R. Millioni, L. Puricelli and R. Orlando, *Curr. Opin. Clin. Nutr. Metab. Care*, 2010, **13**, 81–86.

54 J. Liu, S. Jiang, Y. Zhao, Q. Sun, J. Zhang, D. Shen, J. Wu, N. Shen, X. Fu, X. Sun, D. Yu, J. Chen, J. He, T. Shi, Y. Ding, L. Fang, B. Xue and C. Li, *J. Pathol.*, 2018, **246**, 277–288.

55 E. M. Palsson-McDermott and L. A. O'neill, *BioEssays*, 2013, **35**, 965–973.

56 F. De Chiara, S. Heebøll, G. Marrone, C. Montoliu, S. Hamilton-Dutoit, A. Ferrandez, F. Andreola, K. Rombouts,

H. Grønbæk, V. Felipo, J. Gracia-Sancho, R. P. Mookerjee, H. Vilstrup, R. Jalan and K. L. Thomsen, *J. Hepatol.*, 2018, **69**, 905–915.
57 R. Sun, D. Xu, Q. Wei, B. Zhang, J. Aa, G. Wang and Y. Xie, *Biomed. Pharmacother.*, 2020, **123**, 109721.
58 M. C. Garcia, M. Amankwa-Sakyi and T. J. Flynn, *Toxicol. In Vitro*, 2011, **25**, 1501–1506.
59 D. M. Rocha, A. P. Caldas, L. L. Oliveira, J. Bressan and H. H. Hermsdorff, *Atherosclerosis*, 2016, **244**, 211–215.
60 C. Shen, W. Ma, L. Ding, S. Li, X. Dou and Z. Song, *J. Cell. Mol. Med.*, 2018, **22**, 3572–3581.
61 A. Morris, *Nat. Rev. Endocrinol.*, 2018, **14**, 382.
62 K. M. Ajuwon and M. E. Spurlock, *J. Nutr.*, 2005, **135**, 1841–1846.
63 P. P. Hommelberg, J. Plat, R. C. Langen, A. M. Schols and R. P. Mensink, *Am. J. Physiol.: Endocrinol. Metab.*, 2009, **296**, E114–E120.
64 P. Dey, J. B. Kim, C. Chitchumroonchokchai, J. Li, G. Y. Sasaki, B. D. Olmstead, K. L. Stock, J. M. Thomas-Ahner, S. K. Clinton and R. S. Bruno, *Food Funct.*, 2019, **10**, 6351–6361.
65 K. Miura, L. Yang, N. van Rooijen, D. A. Brenner, H. Ohnishi and E. Seki, *Hepatology*, 2013, **57**, 577–589.
66 N. M. Darwish, M. M. A. Elshaer, S. M. Almutairi, T. W. Chen, M. O. Mohamed, W. B. A. Ghaly and R. A. Rasheed, *Molecules*, 2022, **27**, 3032.
67 X. Yu, W. Peng, Y. Wang, W. Xu, W. Chen, L. Huang, H. Xu, X. He, S. Wang and Q. Sun, *Cancers*, 2023, **15**, 388.
68 L. Lin, Y. Ding, Y. Wang, Z. Wang, X. Yin, G. Yan, L. Zhang, P. Yang and H. Shen, *Hepatology*, 2017, **66**, 432–448.
69 S. Li, M. Hong, H.-Y. Tan, N. Wang and Y. Feng, *Oxid. Med. Cell. Longevity*, 2016, **2016**, DOI: **10.1155/2016/4234061**.
70 Z. Chen, R. Tian, Z. She, J. Cai and H. Li, *Free Radicals Biol. Med.*, 2020, **152**, 116–141.
71 H. Raza, A. John and J. Shafarin, *PLoS One*, 2016, **11**, e0159750.
72 A. I. Rojo, M. Pajares, A. J. García-Yagüe, I. Buendia, F. Van Leuven, M. Yamamoto, M. G. López and A. Cuadrado, *Redox Biol.*, 2018, **18**, 173–180.
73 R. G. R. Mooli, D. Mukhi and S. K. Ramakrishnan, *Compr. Physiol.*, 2022, **12**, 3167–3192.
74 S. Li, H. Y. Tan, N. Wang, Z. J. Zhang, L. Lao, C. W. Wong and Y. Feng, *Int. J. Mol. Sci.*, 2015, **16**, 26087–26124.
75 H. Shi, Y. Guo, Y. Liu, B. Shi, X. Guo, L. Jin and S. Yan, *Anim. Nutr.*, 2016, **2**, 99–104.
76 Z. Spolarics and J.-X. Wu, *Am. J. Physiol.: Gastrointest. Liver Physiol.*, 1997, **273**, G1304–G1311.
77 M. Jia, Y. Jing, Q. Ai, R. Jiang, J. Wan, L. Lin, D. Zhou, Q. Che, L. Li and L. Tang, *Hepatol. Res.*, 2014, **44**, 1151–1158.
78 A. Alnahdi, A. John and H. Raza, *Nutrients*, 2019, **11**, 1979.
79 M. X. Zhao, J. L. Wen, L. Wang, X. P. Wang and T. S. Chen, *Cell Stress Chaperones*, 2019, **24**, 609–619.
80 K. Suriyaprom, S. Kaewprasert, P. Putpadungwipon, P. Namjuntra and S. Klongthalay, *J. Health Popul. Nutr.*, 2019, **38**, 1.
81 K. Verma, S. Makwana, S. Paliwal, V. Paliwal, S. Jain, S. Paliwal and S. Sharma, *Curr. Res. Pharmacol. Drug Discovery*, 2022, **3**, 100088.
82 J. Y. Lee, C. A. Lowell, D. G. Lemay, H. S. Youn, S. H. Rhee, K. H. Sohn, B. Jang, J. Ye, J. H. Chung and D. H. Hwang, *Biochem. Pharmacol.*, 2005, **70**, 1231–1240.
83 S. Deng, K. Yu, B. Zhang, Y. Yao, Z. Wang, J. Zhang, X. Zhang, G. Liu, N. Li, Y. Liu and Z. Lian, *Oxid. Med. Cell. Longevity*, 2015, **2015**, 359315.
84 S. Qiu, Y. Cai, H. Yao, C. Lin, Y. Xie, S. Tang and A. Zhang, *Signal Transduction Targeted Ther.*, 2023, **8**, 132.
85 T. Buergel, J. Steinfeldt, G. Ruyoga, M. Pietzner, D. Bizzarri, D. Vojinovic, J. Upmeier zu Belzen, L. Loock, P. Kittner and L. Christmann, *Nat. Med.*, 2022, **28**, 2309–2320.
86 R. Radi, *Proc. Natl. Acad. Sci. U. S. A.*, 2018, **115**, 5839–5848.
87 N. Krishnan, M. B. Dickman and D. F. Becker, *Free Radicals Biol. Med.*, 2008, **44**, 671–681.
88 S. Sharma, X. Zhang, G. Azhar, P. Patyal, A. Verma, G. Kc and J. Y. Wei, *Biosci., Biotechnol., Biochem.*, 2024, **88**, 168–176.

